A Posteriori Error Estimator for a Multiscale Hybrid Mixed Method Applied to Darcy's Flows

Gustavo A. Batistela, Denise de Siqueira,
Phillipe R. B. Devloo, Sônia M. Gomes
State University of Campinas, Brazil
*S*ummer School on Numerical Analysis - EDF Lab
Paris-Saclay June 27- July 1 , 2022

Motivation

Darcy's flows in heterogeneous porous media have multiscale characteristics due to geological parameters of the rock matrix

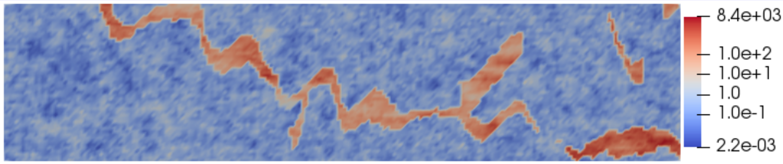

Having limited CPU resources, accurate standard discretizations may be unfeasible

One option: Multiscale Hybrid-Mixed FE method - MHM-H(div)[a]:
at a reduced CPU cost, it incorporates small scale effects (inside macro-elements) onto larger scale fields (H(div)-conforming flux constrained by with coarse normal trace over the mesh skeleton + elementwise average potential)

[a]Durán, Devloo, Gomes, Valentin (2019) *A multiscale hybrid method for Darcy's problems using mixed finite element local solvers*: CMAME, 354: 213–244

Goal: a posteriori estimates for the MHM-H(div) method

1. Provide **computable error bounds** based on the approximate solution: extension to the MHM-H(div) method of known estimators designed for standard mixed FE methods , which are based on a **potential reconstruction procedure**[a][b]

2. **Authomatic h-adaptive algorithm** for the normal trace variable to control a desired accuracy: guided by the computed a posteriori error estimator

3. **Performance evaluation of the error estimator and the adaptive scheme** through a set of illustrating numerical test problems.

---

[a] Vohralík (2010) *Unified primal formulation-based a priori and a posteriori erroranalysis of mixed finite element methods*. Math Comput, 79(272):2001–2032

[b] Ainsworth, Ma (2012) *Non-uniform order mixed FEM approximation: Implementation, post-processing, computable error bound and adaptivity*. J Comput Phys 231: 436–453

Acknowledgements

This study is part of the Research Line 1 - Production Optimization using Reservoir Simulation Models of the joint project ERC-RPM – Unicamp/Equinor/FAPESP

Model problem and mixed formulation

$(\boldsymbol{\sigma}, u)$: flux and potential (pressure) fields in the porous media Ω

$$\boldsymbol{\sigma} = -\mathbb{K}\nabla u, \quad \nabla \cdot \boldsymbol{\sigma} = f, \text{ in } \Omega,$$

$$u = u_D \text{ on } \Gamma_D, \quad \boldsymbol{\sigma} \cdot \boldsymbol{n}^\Omega = \sigma_N \text{ on } \Gamma_N$$

$$u_D \in H^{1/2}(\Gamma_D) \cap C^0(\bar{\Gamma}_D), \sigma_N \in L^2(\Gamma_N)$$

$\mathbb{K}$: bounded symmetric positive definite (permeability) tensor

Find $(\boldsymbol{\sigma}, u) \in H(\mathrm{div};\Omega) \times L^2(\Omega)$, $\boldsymbol{\sigma} \cdot \mathbf{n}^\Omega|_{\Gamma_N} = \sigma_N$ verifying

$$\int_\Omega \mathbb{K}^{-1} \boldsymbol{\sigma} \cdot \mathbf{q}\, dx - \int_\Omega u \nabla \cdot \mathbf{q}\, dx = -\int_{\Gamma_D} u_D(\mathbf{q} \cdot \boldsymbol{n}^\Omega)\, ds,$$

$$\int_\Omega \nabla \cdot \boldsymbol{\sigma}\, v\, dx = \int_\Omega f v\, dx,$$

$\forall \mathbf{q} \in H(\mathrm{div};\Omega), \mathbf{q} \cdot \mathbf{n}^\Omega|_{\Gamma_N} = 0$ and $\forall v \in L^2(\Omega)$.

u: Lagrange multiplier enforcing the divergence constraint

$$H(\mathrm{div};\Omega) = \{\mathbf{q} \in L^2(\Omega, \mathbb{R}^d); \nabla \cdot \mathbf{u} \in L^2(\Omega)\}$$

FE mixed discretizations of Darcy's flows

$\mathcal{T} = \{\Omega_i\}$: **partition of** Ω

FE pair: $(\tilde{\mathbf{V}} \times \tilde{U}) \subset H(\mathrm{div};\Omega) \times L^2(\Omega)$

$$\tilde{\mathbf{V}} = \{\mathbf{q} \in H(\mathrm{div};\Omega); \mathbf{q}|_{\Omega_i} \in \mathbf{V}(\Omega_i),\ \Omega_i \in \mathcal{T}\}$$

$$\tilde{U} = \{v \in L^2(\Omega); v|_{\Omega_i} \in U(\Omega_i)\ \Omega_i \in \mathcal{T}\}$$

Find $(\tilde{\boldsymbol{\sigma}}, \tilde{u}) \in \tilde{\mathbf{V}} \times \tilde{W}$, $\tilde{\boldsymbol{\sigma}} \cdot \mathbf{n}^\Omega|_{\Gamma_N} = \Pi_\gamma^N \sigma_N$ verifying

$$\int_\Omega \mathbb{K}^{-1}\, \tilde{\boldsymbol{\sigma}} \cdot \mathbf{q}\, dx - \int_\Omega \tilde{u}\, \nabla \cdot \mathbf{q}\, dx = -\int_{\Gamma_D} u_D(\mathbf{q} \cdot \boldsymbol{n}^\Omega)\, ds,$$

$$\int_\Omega \nabla \cdot \tilde{\boldsymbol{\sigma}}\, v\, dx = \int_\Omega fv\, dx,$$

$\forall \mathbf{q} \in \tilde{\mathbf{V}}, \mathbf{q} \cdot \mathbf{n}^\Omega|_{\Gamma_N} = 0$ and $\forall v \in \tilde{U}$.

Π_γ^N: L^2-projection on $\Lambda_\gamma^N = \{\nu \in \mathrm{L}^2(\Gamma_N) : \nu|_F = \boldsymbol{\tau} \cdot \mathbf{n}^\Omega|_F,\ \boldsymbol{\tau} \in \tilde{\mathbf{V}}, F \subset \Gamma_N\}$

Divergence-consistency: $\nabla \cdot \tilde{\mathbf{V}} = \tilde{U}$ is required for stability

Why mixed formulation?: optimal flux accuracy, locally conservative approximations, strongly divergence-free simulations

$H(\text{div})$-conforming FE approximations $\tilde{\boldsymbol{\sigma}} \approx \boldsymbol{\sigma}$

Are characterized by continuous normal interface traces: are well known for standard types of element geometry [a]: triangular, quadrilateral, tetrahedral, hexahedral, prismatic

Hierarchical high order shape functions: of trace type or bubbles (vanishing normal traces), can be constructed multiplying appropriate vector fields by scalar H^1-conforming shape functions [b]

Implementation in NeoPZ [c]: hierachy of shape functions in 2D, 3D, and manifolds, tools available for the identification of trace and bubble functions of different degree

---

[a] [1] Fuentes, Keith, Demkowicz, Nagaraj (2015)
[b] [2] Castro, Devloo, Farias, G, de Siqueira (2016)
[c] [3] NeoPZ open source platform: http://github.com/labmec/neopz

Comments on implementation: static condensation

$$\tilde{\mathbf{V}} = \tilde{\mathbf{V}}^{\partial} \oplus \mathring{\tilde{\mathbf{V}}} \quad (\text{trace type} \oplus \text{internal type})$$

$$\tilde{U} = U_0 \oplus \tilde{U}^{\perp} \quad (\text{piecewise constants} \oplus \text{piecewise zero} - \text{mean})$$

$\tilde{\boldsymbol{\sigma}} = \tilde{\boldsymbol{\sigma}}^{\partial} + \mathring{\tilde{\boldsymbol{\sigma}}} \quad \tilde{u} = \bar{\tilde{u}} + \tilde{u}^{\perp}$

$\tilde{\delta} \in U_0$: new multiplier to enforce the solvability constraint $\tilde{u} - \bar{\tilde{u}} \in \tilde{U}^{\perp}$

Primary DoF $\mathbf{V}_1 = (\hat{\boldsymbol{\sigma}}_1, \hat{\bar{u}})^T$: for $(\tilde{\boldsymbol{\sigma}}^{\partial}, \bar{\tilde{u}})$

Secondary DoF $\mathbf{V}_0 = (\hat{\boldsymbol{\sigma}}_0, \hat{p}, \hat{\tilde{\delta}})^T$: for $(\mathring{\tilde{\boldsymbol{\sigma}}}, \tilde{p}, \tilde{\delta})$

Local matrix structure in Ω_i:

$$\left[\begin{array}{c|c} \mathbf{K}^i_{00} & \mathbf{K}^i_{01} \\ \hline \mathbf{K}^i_{10} & \mathbf{K}^i_{11} \end{array}\right] \cdot \left[\begin{array}{c} \mathbf{V}^i_0 \\ \hline \mathbf{V}^i_1 \end{array}\right] = \left[\begin{array}{c} \mathbf{f}^i_0 \\ \hline \mathbf{f}^i_1 \end{array}\right]$$

Condensed(global) system: $\mathbf{K}\mathbf{V}_1 = \mathbf{f}$

$\mathbf{K}$ and $\mathbf{f}$: assembly of $\mathbf{K}^i_{11} - \mathbf{K}^i_{10}\, \mathbf{K}^{i-1}_{00}\, \mathbf{K}^i_{01}$ and $\mathbf{f}^i_1 - \mathbf{K}^i_{01}\, \mathbf{K}^{i-1}_{00} \cdot \mathbf{f}^i_0$

Recovery of $\mathbf{V}_0$ by independent local solvers in Ω_i: $\mathbf{K}^i_{00}\mathbf{V}^i_0 = \mathbf{f}^i_0 - \mathbf{K}^i_{01}\mathbf{V}^i_1$

Focus: trace-constrained $H(\mathrm{div})$-conforming FE spaces

Polytopal partitions: polygonal or polyhedral subregions

Different scale FE space settings: $\tilde{\mathbf{V}} = \tilde{\mathbf{V}}^{\partial} \oplus \mathring{\tilde{\mathbf{V}}}$

- Refined composite FE spaces inside polytopes (in h and/or k): $\mathring{\tilde{\mathbf{V}}}$
- Coarser trace constraints over the mesh skeleton: $\tilde{\mathbf{V}}^{\partial}$

Usefull for [a]: enhancing accuracy [1]; *hp* - adaptivity [2]; Te-H-Pr-P meshes combined in the same simulation [3]

Aplications in MHM-Hdiv methods[b]: Darcy's flows [4] and elasticity [5]

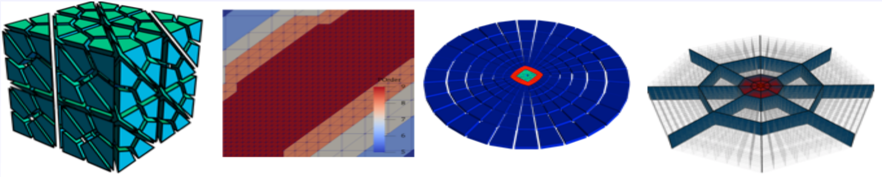

[a] [1] Devloo, Durán, Farias, G (2019); [2] Demkowicz, Monk, Vardapetvan, Rachowicz (2000); [2] Devloo, Durán, G, Ainsworth (2019)

[b] [4] Durán, Devloo, G, Valentin (2019); [5] Devloo, Farias, G, Santos, Pereira, Valentin (2021)

Two-scale settings $\mathcal{E}_\gamma$: about the meshes

$$\mathcal{E}_\gamma = \mathbf{V}_\gamma \times U_{\gamma_{in}}$$

Discretization parameters: $\gamma = (\gamma_{sk}, \gamma_{in})$ coarse and fine scales

$$\gamma_{sk} = (h_{sk}, k_{sk}), \quad \gamma_{in} = (h_{in}, k_{in})$$

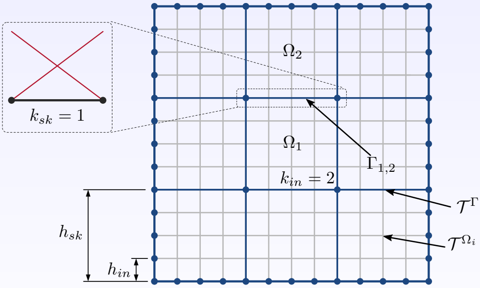

$\mathcal{T} = \{\Omega_i\}$ macro-partition
$\mathcal{T}^{\Omega_i} = \{K\}$ refined local partitions by micro-elements K (may be non-conformal over $\partial\Omega_i \cap \partial\Omega_j$)

Γ skeleton
$\mathcal{T}^\Gamma$ coarse skeleton mesh:
mesh consistency: the mesh induced by $\mathcal{T}^{\Omega_i}$ on $\partial\Omega_i$ is a refinement of $\mathcal{T}^\Gamma|_{\partial\Omega_i}$

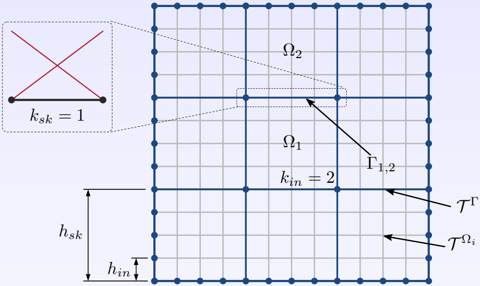

$\mathbf{V}_{\gamma_{in}}(\Omega_i) \times W_{\gamma_{in}}(\Omega_i)$: refined FE pairs

Λ_γ: coarse normal trace FE space:
consistency: $\Lambda_\gamma|_{\partial\Omega_i} \subset \mathbf{V}_{\gamma_{in}}(\Omega_i) \cdot \boldsymbol{n}^{\Omega_i}|_{\partial\Omega_i}$:

$\mathbf{V}_\gamma(\Omega_i) \subset \mathbf{V}_{\gamma_{in}}(\Omega_i)$ two-scale subspace constrained to Λ_γ

$\mathbf{V}_\gamma(\Omega_i) = \mathbf{V}^\partial_\gamma(\Omega_i) \oplus \mathring{\mathbf{V}}_{\gamma_{in}}(\Omega_i)$

Local communication of constrained normal trace fluxes on $\partial\Omega_i \cap \partial\Omega_j$ affects at most two neighbouring layers of micro-elements

Reduced global system (i.e. coarser primary DoF) whilst accuracy is locally preserved using refined local secondary variables

MHM-H(div)($\mathcal{E}_\gamma$): a priori error estimates

$$\mathbf{V}_\gamma = \{\mathbf{q} \in H(\mathrm{div};\Omega); \mathbf{q}|_{\Omega_i} \in \mathbf{V}_\gamma(\Omega_i),\ \Omega_i \in \mathcal{T}\}$$
$$U_{\gamma_{in}} = \{v \in L^2(\Omega); v|_{\Omega_i} \in U_{\gamma_{in}}(\Omega_i)\ \Omega_i \in \mathcal{T}\}$$

MHM-H(div)($\mathcal{E}_\gamma$): FE mixed formulation based on $\mathcal{E}_\gamma = \mathbf{V}_\gamma \times U_{\gamma_{in}}$

A priori estimates for $\boldsymbol{\sigma} - \tilde{\boldsymbol{\sigma}}$ and $u - \tilde{u}$: are usually obtained in terms of the error $\boldsymbol{\sigma} - \boldsymbol{\Pi}_\gamma^D \boldsymbol{\sigma}$ for a projection $\boldsymbol{\Pi}_\gamma^D : H^s(\Omega, \mathbb{R}^d) \to \mathbf{V}_\gamma$ commuting the divergence operator

$$\begin{array}{ccc} \mathbf{H}^1(\mathrm{div}, \Omega) \subset \mathbf{H}(\mathrm{div}, \Omega) & \xrightarrow{\nabla\cdot} & L^2(\Omega) \\ \downarrow \boldsymbol{\Pi}_\gamma^D & & \downarrow \Pi^{L^2} \\ \mathbf{V}_\gamma & \xrightarrow{\nabla\cdot} & U_{\gamma_{in}} \end{array}$$

Convergence rates: depend on:

a) regularity of the exact fields $(\boldsymbol{\sigma}, p)$;

b) capacity of FE spaces to reproduce polynomials

General a priori error estimates for MHM-H(div)($\mathcal{E}_\gamma$)

Theorem

Suppose the exact fields are regular enough, and $(\tilde{\boldsymbol{\sigma}}, \tilde{u})$ are approximate solutions by the MHM-H(div)($\mathcal{E}_\gamma$) method, and the elliptic regularity property is valid. If $\mathbb{P}_k(K, \mathbb{R}^d) \subset \mathbf{V}(K)$, and $\mathbb{P}_{k+t}(K) \subset U(K)$, then

$$\|\boldsymbol{\sigma} - \tilde{\boldsymbol{\sigma}}\|_{\mathbf{L}^2(\Omega,\mathbb{R}^d)} \lesssim h_{sk}^{k_{sk}+1} \|\boldsymbol{\sigma}\|_{\mathbf{H}^{k_{sk}+1}(\Omega,\mathbb{R}^d)}$$

$$\|\nabla \cdot (\boldsymbol{\sigma} - \tilde{\boldsymbol{\sigma}})\|_{L^2(\Omega)} \lesssim h_{in}^{k_{in}+t+1} \|\boldsymbol{\nabla} \cdot \boldsymbol{\sigma}\|_{H^{k_{in}+t+1}(\Omega)}$$

$$\|u - \tilde{u}\|_{L^2(\Omega)} \lesssim h_{sk}^{k_{sk}+2} \|\boldsymbol{\sigma}\|_{\mathbf{H}^{k_{sk}+1}(\Omega,\mathbb{R}^d)} + h_{in}^{k_{in}+t+1} \|u\|_{H^{k_{in}+t+1}(\Omega)}$$

Leading constants (unknown): depend only on the shape-regularity of the partition (independent of the fields and discretization parameters)

Useful for qualitative assymptotic convergence behaviour of the method

Convergence rates deteriorate for irregular solutions: adaptivity is a remedy

Smooth solution: affine hexahedra, tetrahedra, or prisms [4]

$$\Omega = (0,1)^3,\ f = -\Delta u_{exact},\ \text{and}\ u_D = u_{exact}\big|_{\partial\Omega},$$

$$u_{exact} = \frac{\pi}{2} - \tan^{-1}\left(5\left(\sqrt{(x-1.25)^2 + (y+0.25)^2 + (z+0.25)^2} - \frac{\pi}{3}\right)\right)$$

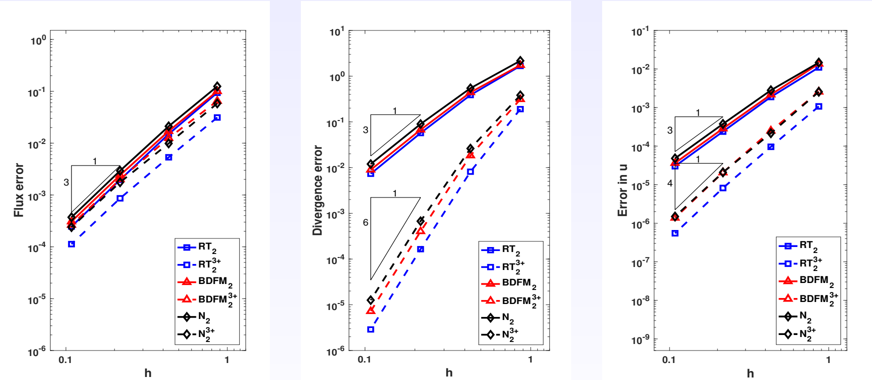

$k_{sk} = 2,\ k_{in} = k_{sk} + n,\ n = 0$ (continuous), 3 (dashed); $h_{in} = h_{sk} = h$

[4] Devloo, Durán, Farias, G (2018), IJNME

MHM-H(div): flow around a vertical well [8]

Heterogeneous media; expected singular behaviour close to the well

h-Adaptive MHM macro-partition at level ℓ: $h^i_{sk}(\ell) = H^i/2^\ell$, $h_{in} = H^i/2^3$

local FE pair RT_1; $k_{sk} = 1$

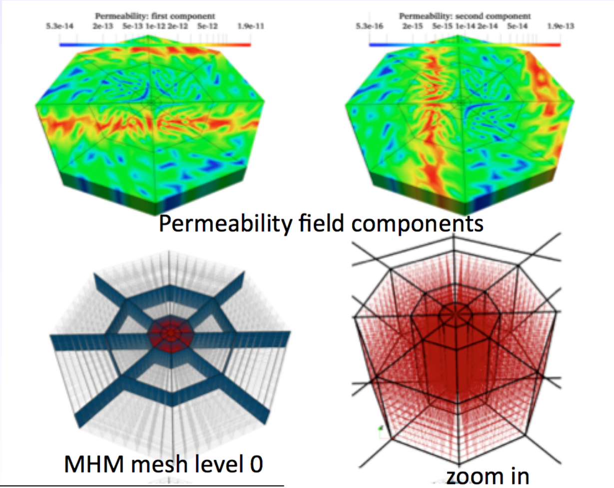

[6] Durán, Devloo, G, Valentin (2019) CMAME

MHM-H(div) for radial flow

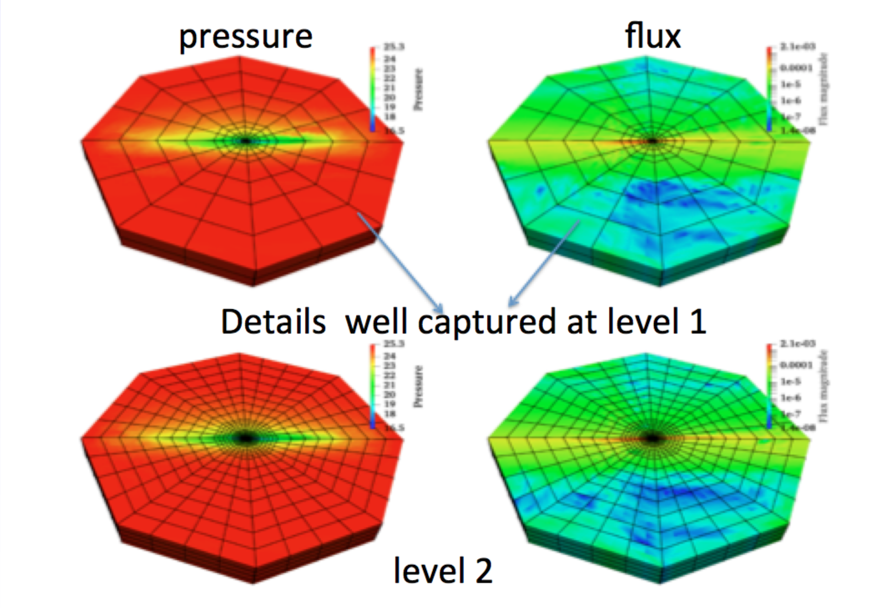

A posteriory error estimators

Should be computable from $(\tilde{\boldsymbol{\sigma}}, \tilde{u})$ and problem data (f, u_D, σ_N)
Should be efficient: close to the (unknown) exact errors
Useful to guide the design of authomatic adaptive discretizations

Synthetic benchmark reservoir model by UNISIM-CEPETRO-Unicamp [a]

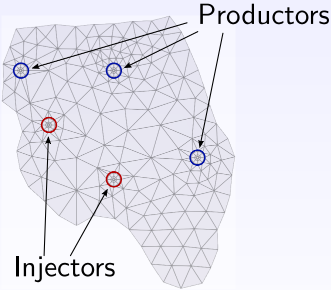

macro partition

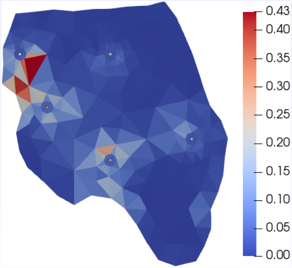

error indicators

[a] https://www.unisim.cepetro.unicamp.br/benchmarks/br/

Potential reconstruction

exact u

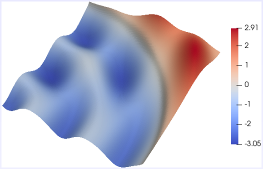

$\tilde{u}$

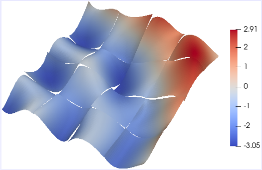

Potential reconstruction: is a potential $s \in H^1(\Omega) \cap C(\bar{\Omega})$, $s|_{\Gamma_D} = \mu$

$\mu|_{\Gamma_D} \approx u_D$: continuous piecewise polynomial over the partition $\mathcal{T}^{\Gamma}|_{\bar{\Gamma}_D}$.

computing $\mu \in C(\Gamma)$

average on edges

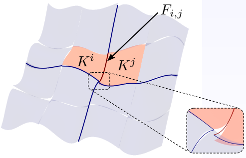

update vertex values

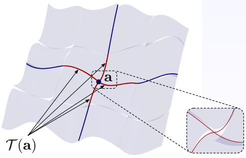

solving local Dirichlet bvp

s

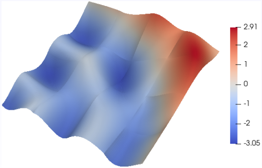

A posteriori error estimates via potential reconstruction

Theorem Let $(\tilde{\boldsymbol{\sigma}}, \tilde{u}) \in \boldsymbol{V}_\gamma \times U_{\gamma_{in}}$ be the solution of the MHM-H(div)-$\mathcal{E}_\gamma$ method, and assume the Poincaré and trace inequalities hold on the subregions Ω_i with computable constants. If $s \in H^1(\Omega) \cap U_{\gamma_{in}}$ is a potential reconstruction, then

$$\|\boldsymbol{\sigma} - \tilde{\boldsymbol{\sigma}}\|^2_{\mathbb{K}^{-1}} \leq \sum_{\Omega_i} (\eta^{(a)}_{\Omega_i})^2 + (\eta^{(b)}_{\Omega_i})^2,$$

for $\eta^{(a)}_{\Omega_i} = \eta_{P,\Omega_i} + \eta_{D,\Omega_i}$, with $\eta_{P,\Omega_i} := \|\mathbb{K}\nabla s + \tilde{\boldsymbol{\sigma}}\|_{\Omega_i,\mathbb{K}^{-1}}$,
$\eta_{D,\Omega_i} := \min_{w \in \mathrm{H}^1_{u_D,\mu}(\Omega_i)} \|\mathbb{K}\nabla w\|_{\Omega_i,\mathbb{K}^{-1}}$, and $\eta^{(b)}_{\Omega_i} = \eta_{R,\Omega_i} + \eta_{N,\Omega_i}$, with

$$\eta_{R,\Omega_i} := \frac{\delta_{\Omega_i} C_{P,\Omega_i}}{\sqrt{C_{\mathbb{K},\Omega_i}}} \|f - \Pi_{\gamma_{in}} f\|_{L^2(\Omega_i)},$$

$$\eta_{N,\Omega_i} := \frac{\left[C_{\mathrm{tr},\Omega_i} C_{P,\Omega_i} \delta_{\Omega_i} \left(d C_{P,\Omega_i} + 2\right)\right]^{1/2}}{\sqrt{C_{\mathbb{K},\Omega_i}}} \|\sigma_N - \Pi_{N,\gamma_{in}} \sigma_N\|_{L^2(\partial\Omega_i \cap \Gamma_N)}$$

$\mathrm{H}^1_{u_D,\mu}(\Omega_i) = \{w \in \mathrm{H}^1(\Omega_i) : w|_{\Gamma_D \cap \Omega_i} = u_D - \mu,\ w|_{\Omega_i \setminus \Gamma_D} = 0\}$

$||\boldsymbol{\tau}||_{\mathbb{K}^{-1}} = \int_\Omega \mathbb{K}^{-1} \boldsymbol{\tau} \cdot \boldsymbol{\tau}\, d\boldsymbol{x}$: energy norm

Computable leading constants in $\eta^{(b)}_{\Omega_i}$

Poincaré inequality: There exists a constant $C_{P,\mathcal{R}} > 0$ such that

$$\|\varphi - \varphi_0\|_{L^2(\mathcal{R})} \leq C_{P,\mathcal{R}} \delta_{\mathcal{R}} \|\nabla \varphi\|_{L^2(\mathcal{R})}, \quad \forall \varphi \in H^1(\mathcal{R})$$

where φ_0 is the average of φ in $\mathcal{R}$ and $\delta_{\mathcal{R}}$ is the diameter of $\mathcal{R}$.

$C_{P,\mathcal{R}} = \pi^{-1}$ if $\mathcal{R}$ is convex

Trace inequality[a]: There exists a constant $C_{\mathrm{tr},\mathcal{R}} > 0$ such that

$$\|\varphi\|^2_{L^2(\partial\mathcal{R})} \leq C_{\mathrm{tr},\mathcal{R}} \left(\frac{d}{\delta_{\mathcal{R}}} \|\varphi\|_{L^2(\mathcal{R})} + 2\|\nabla \varphi\|_{L^2(\mathcal{R})} \right) \|\varphi\|_{L^2(\mathcal{R})}, \quad \forall \varphi \in H^1(\mathcal{R}$$

If $\mathcal{R}$ is a polytope and $\mathcal{T}^{\mathcal{R}} = \{T\}$ is a matching shape-and contact-regular simplicial sub-partition, then $C_{\mathrm{tr},\mathcal{R}} = (d+1)\frac{C_{\mathrm{tr},\mathcal{T}_{\mathcal{R}}}}{\varrho_{\mathcal{R}}}$, where $C_{\mathrm{tr},\mathcal{T}_{\mathcal{R}}} := \min_{T \in \mathcal{T}^{\mathcal{R}}} C_{\mathrm{tr},T}$, and $\varrho_{\mathcal{R}} := \frac{\min_{T\in\mathcal{T}^{\mathcal{R}}} \delta_T}{\delta_{\mathcal{R}}}$

[a] Di Pietro, Ern - Mathematical aspects of DG methods, Springer 2012

$C_{\mathbb{K},\Omega_i}$: smallest eigenvalues of $\mathbb{K}$ on Ω_i

Remarks

η_{P,Ω_i}, η_{N,Ω_i}, and η_{R,Ω_i}: are fully computable in terms of the $(\tilde{\boldsymbol{\sigma}}, \tilde{u})$, s, f, σ_N

η_{P,Ω_i}: measures error in the approximation $\tilde{\boldsymbol{\sigma}} \approx -\mathbb{K}\nabla s$ in Ω_i
Most significant error indicator

η_{R,Ω_i}: measures the residual error $(f - \Pi_{\gamma_{in}} f)|_{\Omega_i}$, is $O(h_{in}^{k_{in}+1})$ for smooth f

η_{N,Ω_i}: reflects the error $(\sigma_N - \Pi_{N,\gamma_{in}} \sigma_N)|_{\Gamma_N \cap \partial\Omega_i}$. Thus, $\eta_{N,\Omega_i} = 0$ for $\Gamma_N = \emptyset$, $\sigma_N = 0$, or for $\sigma_N \in \Lambda_\gamma|_{\Gamma_N}$. It is $O(h_{in}^{k_{in}+1})$ for smooth σ_N.

η_{D,Ω_i}: In general, it is is not computable; measures the error $(u_D - \mu)|_{\Gamma_D}$: thus it vanishes if $u_D = \mu|_{\Gamma_D}$ is a continuous piecewise polynomial function, and decays fast for smooth u_D. Estimates of η_{D,Ω_i} available in 2D[a]

[a] Dolejší, Ern, Vohralík, hp-adaptation driven by polynomial-degree-robust a posteriori error estimates for elliptic problems. SIAM J Sci Comput 2016; 38: A3220-A3246

Outline of the proof: following [1]

Auxiliary fields $(\bar{\boldsymbol{\sigma}}, \bar{u}) \in H(\mathrm{div}, \Omega) \times L^2(\Omega)$ solving the model problem with $\bar{\boldsymbol{\sigma}} \cdot \mathbf{n}^{\Omega} = \Pi_{N,\gamma_{in}} \sigma_N$, $\bar{u}|_{\Gamma_D} = u_D$ and f replaced by $\Pi_{\gamma_{in}} f$.

Lemma 1 : $\|\bar{\boldsymbol{\sigma}} - \tilde{\boldsymbol{\sigma}}\|^2_{\mathbb{K}^{-1}} = \min\limits_{\substack{v \in \mathrm{H}^1(\Omega) \\ v|_{\Gamma_D} = u_D}} \|\mathbb{K}\nabla v + \tilde{\boldsymbol{\sigma}}\|^2_{\mathbb{K}^{-1}}$

Lemma 2 (Pythagoras): $\|\boldsymbol{\sigma} - \tilde{\boldsymbol{\sigma}}\|^2_{\mathbb{K}^{-1}} = \|\bar{\boldsymbol{\sigma}} - \tilde{\boldsymbol{\sigma}}\|^2_{\mathbb{K}^{-1}} + \|\boldsymbol{\sigma} - \bar{\boldsymbol{\sigma}}\|^2_{\mathbb{K}^{-1}} = (a) + (b)$

First estimation: $(a) \le \sum_{\Omega_i} (\eta_{P,\Omega_i} + \eta_{D,\Omega_i})^2$

$$(a) \le \sum_{\Omega_i \in \mathcal{T}} (\|\mathbb{K}\nabla s + \tilde{\boldsymbol{\sigma}}\|_{\Omega_i,\mathbb{K}^{-1}} + \min_{w \in \mathrm{H}^1_{\mathrm{u_D},\mu}(\Omega_\mathrm{i})} \|\mathbb{K}\nabla(w)\|_{\Omega_i,\mathbb{K}^{-1}})^2$$

Second estimation: $(b) \le I_1 + I_2 \le \sum_{\Omega_i} (\eta_{R,\Omega_i} + \eta_{N,\Omega_i})^2$

$$I_1 = \sum_{\Omega_i} \int_{\Omega_i} (u - \bar{u})(f - \Pi_{\gamma_{in}} f)\, d\mathbf{x} \le \sum_{\Omega_i} \eta_{R,\Omega_i} \|\boldsymbol{\sigma} - \bar{\boldsymbol{\sigma}}\|_{\mathbb{K}^{-1},\Omega_i}$$

$$I_2 = \sum_{\Omega_i} \int_{\partial\Omega_i \cap \Gamma_N} (\bar{u} - u)(\sigma_N - \Pi_{\gamma_{in}} \sigma_N)\, ds \le \sum_{\Omega_i} \eta_{N,\Omega_i} \|\boldsymbol{\sigma} - \bar{\boldsymbol{\sigma}}\|_{\mathbb{K}^{-1},\Omega_i}$$

[1] Ainsworth and Ma (2012)

Verification test problems: known solutions

$\mathcal{T}^{\Omega_i}$: uniform quad; RT: $\mathbf{V}(\hat{K}) = \mathbb{Q}_{m+1,m} \times \mathbb{Q}_{m,m+1}(\hat{K})$, $U(\hat{K}) = \mathbb{Q}_{m,m}(\hat{K})$, $m = k_{in}$; Trace FE: $W(\hat{F}) = \mathbb{P}_{k_{sk}}(\hat{F})$

Exact $E_{\mathrm{ex}} = \|\boldsymbol{\sigma} - \tilde{\boldsymbol{\sigma}}\|_{\mathbb{K}^{-1}}$ and estimated E_{est} errors (and their local versions)

Global and local effectivity indexes: $I_{eff} = \dfrac{E_{\mathrm{est}}}{E_{\mathrm{ex}}}$, $I_{eff}(\Omega_i) = \dfrac{E_{\mathrm{est}}(\Omega_i)}{E_{\mathrm{ex}}(\Omega_i)}$

Case 1

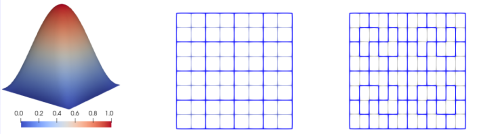

(a) $u(x, y)$ (b) Square subregions (c) L-shaped subregions

$\mathcal{K} = \mathbb{I}$, full $u_D = 0$

Estimators η_P and η_R

Effect of non-convex subregions

Exact versus estimated errors

Case 2

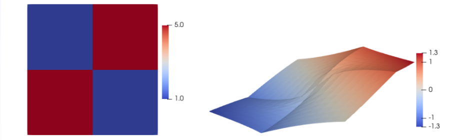

Permeability $u(r, \theta)$

Full u_D, $f = 0$

Effect of discontinuous permeability of the point singularity

$E_{est} = \eta_P$

Smooth solution: Case 1

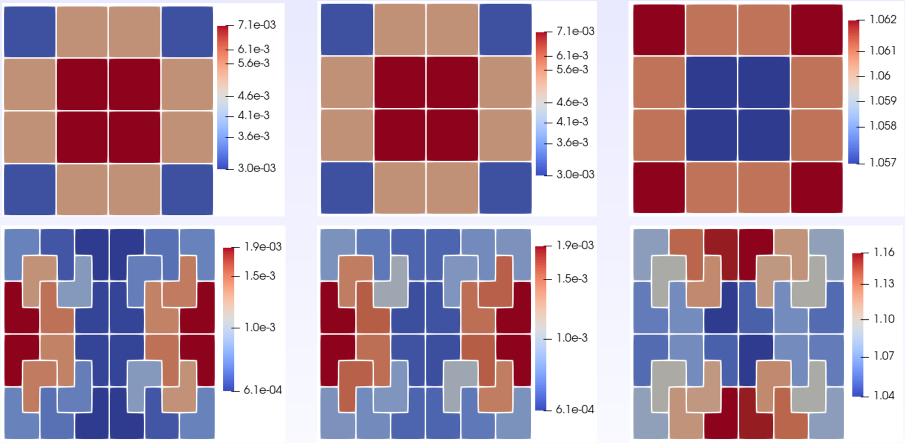

$E_{\mathrm{ex}}(\Omega_i)$ $\quad$ $\eta_{P,\Omega_i} = \|\mathbb{K}\nabla s + \tilde{\boldsymbol{\sigma}}\|_{\Omega_i,\mathbb{K}^{-1}}$ $\quad$ $I_{eff}(\Omega_i)$

Global $I_{eff} = 1.059$ for square and $I_{eff} = 1.09$ for L-shaped subdomains

Convergence history and global efectivity index

Case 1: smooth

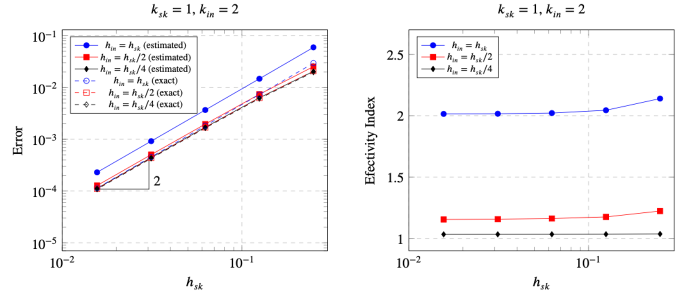

Case 2: center point singularity

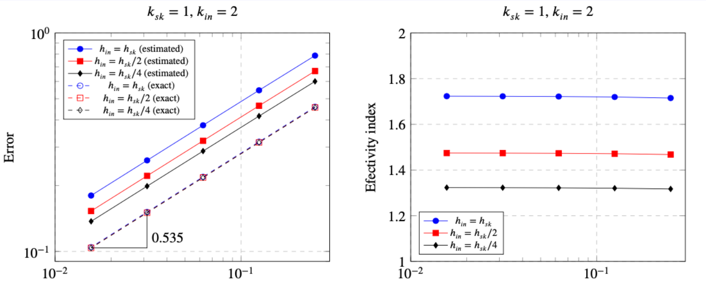

Authomatic Trace h-adaptivity

Fixed geometry (usually given by geologists): conformal partition $\mathcal{T}_{\text{ref}} = \{K\}$ of mesh size h_{in}; Subregions Ω_i by conglomeration of elements K: $\mathcal{T}^{\Omega_i}$;
Fixed polynomial degrees k_{sk} and k_{in}, $k_{sk} \leq k_{in}$
Set coarsest skeleton mesh $\mathcal{T}^{\Gamma,0}$: by the facets of $\partial\Omega_i$ of mesh size h_{sk} and form $\mathcal{E}_\gamma$

Goal: sequence of h_{sk}-refined skeleton meshes $\mathcal{T}^{\Gamma,\ell}$ guided by error indicators η_{P,Ω_i} of the apprpoximate solution of step $\ell - 1$

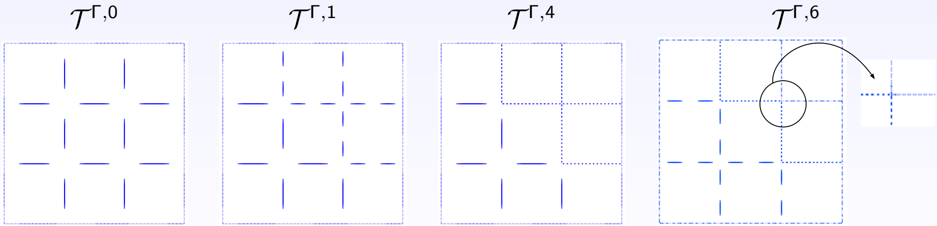

Inside the subregions the meshes are kept at the finest refinement level h_{in}

Trace h-adaptivity (A1)

Input target estimated error η_{goal}, maximum number of iterations *maxiter*, maximum refinement level n_{max}; set $n_{\Omega_j} = 0$, threshold ϵ.

While $\eta > \eta_{goal}$ and iter $<$ *maxiter*:

1. Solve the problem using MHM-H(div)-$\mathcal{E}_\gamma$ method.
2. Compute the error indicator η_{P,Ω_i} associated to the subregions Ω_i.
3. Set $\eta_{\max} = \max_{\Omega_i}\{\eta_{P,\Omega_i} | n_{\Omega_i} < n_{max}\}$. If $\eta_{P,\Omega_i} > \epsilon \cdot \eta_{\max}$ and $n_{\Omega_i} < n_{max}$, increment n_{Ω_i}.
4. Refine $\mathcal{T}^\Gamma$, such that the refinement level of $F_{i,j} = \partial\Omega_i \cap \partial\Omega_j$ is equal to $\max(n_{\Omega_i}, n_{\Omega_j})$. Update $\mathbf{h}_{sk}$ (and γ as well).
5. Update Λ_γ and $\mathbf{V}_\gamma$ constrained to it, and proceed to a new interaction.

Standard subregion h-adaptivity (A2) (for comparison)

Input : initial $\mathcal{E}_\gamma$, $\epsilon \in (0,1)$, η_{goal}, and *maxiter*.

While $\eta > \eta_{goal}$ and iter $<$ *maxiter*:

1. Solve the problem using MHM-H(div)-$\mathcal{E}_\gamma$ method.
2. Compute the error indicator η_{P,Ω_i} associated with each subregions Ω_i.
3. Define $\eta_{\max} = \max_{\Omega_i}\{\eta_{P,\Omega_i}\}$. If $\eta_{P,\Omega_i} > \epsilon \cdot \eta_{\max}$, mark Ω_i to be refined.
4. Refine $\mathcal{T}$ and create $\mathcal{T}^\Gamma$ keeping mesh consistency, and update $\mathbf{h}_{in}$, $\mathbf{h}_{sk}$, and γ, accordingly.
5. Create a new FE space setting $\mathcal{E}_\gamma$ and proceed to a new interaction.

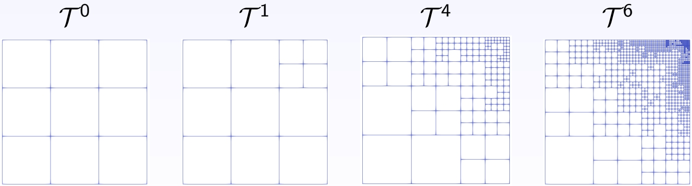

Corner singularity: comparison of adaptive strategies

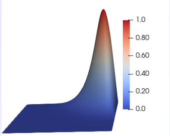

$\mathcal{K} = \mathbb{I}$, full $u_D = 0$

$u(x, y) = xy(1 - x)(1 - y)e^{10x+10y}/537930$

(A1) - trace h-adpativity; (A2) - standard element h-adaptivity; $\epsilon = 0.2$

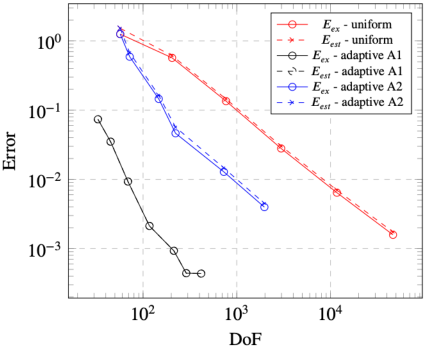

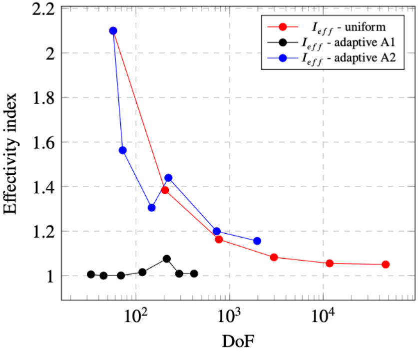

Flow in heterogeneous porous media: trace adaptivity

SPE10 benchmark problem on $\Omega = [0, 208] \times [0, 48]$

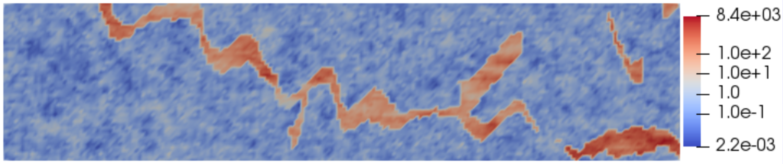

Fixed geometry and parameters: $\mathcal{T}^0 = 13 \times 3$ of square subregions Ω_i; fully refined $\mathcal{T}_{h_{in}}^{\Omega_i}$ ($h_{in} = 1$). $\mathcal{E}_\gamma$ are for $k_{sk} = 1$, $k_{in} = 4$.

$\mathcal{T}^0$ and η_{P,Ω_i}

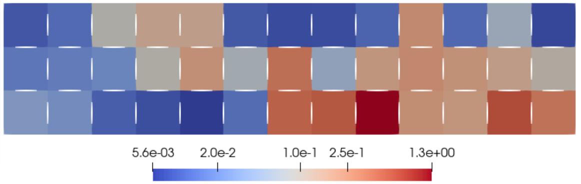

Flow in heterogeneous porous media: trace adaptivity

$\mathcal{T}^{\Gamma,3}$ and η_{P,Ω_i}

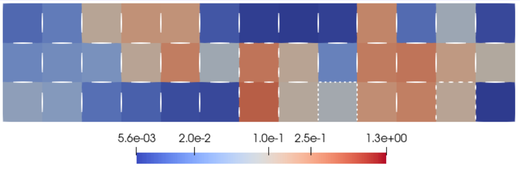

$\mathcal{T}^{\Gamma,6}$ and η_{P,Ω_i}

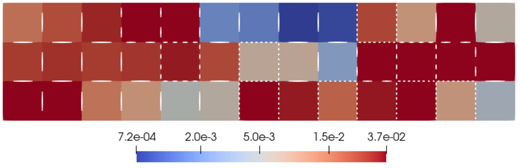

$\mathcal{T}^{\Gamma,8}$and η_{P,Ω_i}

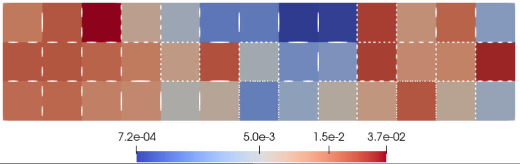

Flow in heterogeneous porous media: a posteriori errors

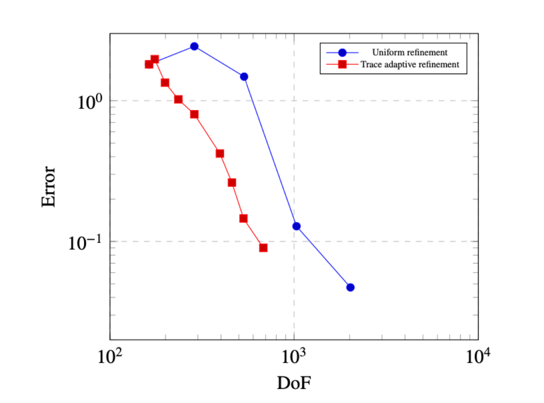

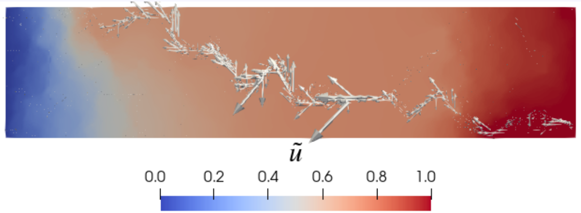

Conclusions

Derivation of a posteriori error estimator for a multiscale hybrid-mixed method for Darcy's flows

The quality of the effectivity index of the error estimator is verified for both convex and non-convex macro domains and is also for problems with smooth and irregular solutions

The estimated error distribution in the macro-domains is used to adaptively refine the skeleton mesh

The adaptivity effectiveness is demonstrated by comparing the error in the energy norm as a function of the size of the global system of equations (DoF)